

Electronic Supplementary Material (ESI) for New Journal of Chemistry. This journal is © The Royal Society of Chemistry and the Centre National de la Recherche Scientifique 2022

## Investigation of Changes Regularities in the Valence State during the Formation of Supported Palladium-Bismuth Nanoparticles by XPS Method

Corresponding Author:

Irina A. Kurzina – Faculty of Chemistry, National Research Tomsk State University, Tomsk, 634050 Russia;

E-mail address: [kurzina99@mail.ru](mailto:kurzina99@mail.ru); Tel.: +7-913-882-1028;

Authors:

Mariya P. Sandu – Department of Chemistry, Siberian State Medical University, Tomsk 634050, Russia;

Faculty of Chemistry, National Research Tomsk State University, Tomsk, 634050 Russia; E-mail address:

[mpsandu94@gmail.com](mailto:mpsandu94@gmail.com). Tel.: +7-953-915-69-71.

Maxim S. Syrtanov – Division for Experimental Physics, National Research Tomsk Polytechnic University,

634050 Tomsk, Russia; E-mail address: [maxim-syrtanov@mail.ru](mailto:maxim-syrtanov@mail.ru). Tel.: +7-952-897-87-86.

Sergey A. Orlov – Faculty of Physics and Engineering, National Research Tomsk State University, 634050

Tomsk, Russia; E-mail address: [orlovtsu@gmail.com](mailto:orlovtsu@gmail.com)

### X-ray photoelectron spectroscopy (XPS)

XPS patterns were obtained using a PHI 5000 VersaProbe-II (ULVAC-PHI, Chigasaki, Kanagawa, Japan). The Al 2p line was taken as an internal standard at 74.5 eV during the analysis of  $\gamma$ -Al<sub>2</sub>O<sub>3</sub>. The accuracy of binding energy measurements was 0.1 kV. The XPS spectra were processed using standard CasaXPS software (version 2.3.22PR1.0, 2018, Casa Software Ltd, UK).

### Transmission electron microscopy and energy (TEM)

JEOL JEM-2100F (JEOL Ltd, Akishima, Tokyo, Japan) was used to obtain TEM-images of the catalysts obtained. The microscope was equipped with an electron gun with the field emission of the cathode (FEG), a high-resolution pole tip (point resolution of 0.19 nm). The samples were suspended in ethanol using an ultrasonic bath and afterwards deposited on the carbon coated copper TEM-grids (3.05 mm in diameter, 300 mesh).

### Scanning electron microscopy and energy dispersive spectroscopy (SEM-EDS)

SEM-images were made using a Tescan MIRA 3 equipped with an energy dispersive spectrometer Oxford Instruments Ultim Max 40 at an accelerating voltage of 20 kV. The equipment was provided by the Analytical Center of Natural Systems' Geochemistry, TSU.

### X-ray diffraction (XRD)

Diffraction patterns were obtained using a diffractometer XRD-7000S (Shimadzu, Kyoto, Japan) in a Bragg-Brentano configuration with CuK<sub>α</sub>-radiation (wavelength  $\lambda = 1.54 \text{ \AA}$ ) at 40 kV and 30 mA. OneSight

1280-channel high-speed detector was used to collect the diffracted radiation. The scanning parameters were as follows:  $2\theta$  range – 10–90°; scan speed – 10.0°/min; sampling pitch – 0.0143°; exposure time – 21.49 s. The PDF4+ 2021 database and Sieve software were used to identify phase composition of the samples.

### Support

Microspherical  $\gamma$ -Al<sub>2</sub>O<sub>3</sub> (“SKTB Katalizator”, Russia) with a surface area of 174 m<sup>2</sup> g<sup>-1</sup> and a total pore volume of 0.35 cm<sup>3</sup> g<sup>-1</sup> was used as a support. The alumina powder was sifted to obtain a particle fraction of 125–250  $\mu$ m.

### Samples characteristics

Table S1 - Characteristics of obtained samples

Sample	Pd content, wt %	Bi content, wt %	Pd/Bi atomic ratio	Specific surface area, m <sup>2</sup> /g	Total pore volume cm <sup>3</sup> /g	Average pore size, nm
Pd/Al <sub>2</sub> O <sub>3</sub>	1.3	-	--	Not measured		
Bi/Al <sub>2</sub> O <sub>3</sub>	-	2.0	--			
Pd3:Bi1/Al <sub>2</sub> O <sub>3</sub>	3.5	2.4	2.9	135	0.26	7.8
Pd5:Bi2/Al <sub>2</sub> O <sub>3</sub>	2.8	2.3	2.4	137	0.26	7.7
Pd1:Bi1/Al <sub>2</sub> O <sub>3</sub>	2.3	4.3	1.0	133	0.27	8.1
Pd1:Bi2/Al <sub>2</sub> O <sub>3</sub>	1.1	3.9	0.6	129	0.25	7.7

Table S2 - XPS analysis results after first step of sample preparation

Sample Pd:Bi	Pd 3d <sub>5/2</sub> , eV	Part, %	Bi 4f <sub>7/2</sub> , eV	Part, %	Pd:Bi
3:1	Pd <sup>0</sup> 334.6	46.3	Bi <sup>0</sup> 156.6	51.9	1.71
	Pd(II) 335.7	53.7	Bi(III) 158.8	48.1	
5:2	Pd <sup>0</sup> 334.6	40.0	Bi <sup>0</sup> 156.6	34.3	1.53
	Pd(II) <sub>ads</sub> 335.5	60.0	Bi(III) 158.5	65.7	
1:1	Pd <sup>0</sup> 334.6	40.0	Bi <sup>0</sup> 156.7	23.0	0.89
	Pd(II) <sub>ads</sub> 335.7	60.0	Bi(III) 158.6	77.0	
1:2	Pd <sup>0</sup> 334.5	19.6	Bi <sup>0</sup> 156.5	42.9	0.36
	Pd(II) <sub>ads</sub> 335.6	80.4	Bi(III) 158.6	57.1	

Table S3 - XPS analysis results after argon treatment of bimetallic samples (500 °C)

Sample Pd:Bi	Pd 3d <sub>5/2</sub> , eV	Part, %	Bi 4f <sub>7/2</sub> , eV	Part, %	Pd:Bi
3:1	Pd <sup>0</sup> 334.7	69.0	Bi <sup>0</sup> 156.5	69.6	2.55
	Pd(II) <sub>ads</sub> 336.3	31.0	Bi(III) <sub>ads</sub> 158.1	30.4	
5:2	Pd <sup>0</sup> 334.6	55.9	Bi <sup>0</sup> 156.8	36.8	1.42
	Pd(II) <sub>ads</sub> 336.3	44.1	Bi(III) 158.4	63.2	
1:1	Pd <sup>0</sup> 334.4	50.4	Bi <sup>0</sup> 156.8	90.2	0.49
	Pd(II) <sub>ads</sub> 336.2	49.6	Bi(III) <sub>ads</sub> 158.0	9.8	
1:2	Pd <sup>0</sup> 334.6	63.1	Bi(III) <sub>ads</sub> 157.6	66.6	0.22
	Pd(II) <sub>ads</sub> 335.9	36.9	Bi(III) 158.5	33.4	

Table S4 - XPS analysis results after oxygen treatment of bimetallic samples (350 °C)

Sample Pd:Bi	Pd 3d <sub>5/2</sub> , eV	Part, %	Bi 4f <sub>7/2</sub> , eV	Part, %	Pd:Bi
3:1	Pd <sup>0</sup> absent Pd(II) <sub>ads</sub> 335.6 Pd(II) 338.1	0 66.2 33.8	Bi(III) <sub>ads</sub> 157.5 Bi(III) 158.8	57.8 42.2	1.96
5:2	Pd <sup>0</sup> 334.7 Pd(II) <sub>ads</sub> 335.6 Pd(II) 337.6	4.9 62.3 32.8	Bi(III) <sub>ads</sub> 157.2 Bi(III) 158.8	29.1 70.9	1.81
1:1	Pd <sup>0</sup> 334.7 Pd(II) <sub>ads</sub> 335.8 Pd(II) 337.5	13.4 74.6 12.0	Bi(III) <sub>ads</sub> 157.4 Bi(III) 158.8	14.9 85.1	0.41
1:2	Pd <sup>0</sup> 334.7 Pd(II) <sub>ads</sub> 335.6 Pd(II) 337.5	15.5 66.3 18.2	Bi(III) <sub>ads</sub> 157.2 Bi(III) 158.5	13.6 87.4	0.25

Table S5 - XPS analysis results after hydrogen treatment of bimetallic samples (500 °C)

Sample Pd:Bi	Pd 3d <sub>5/2</sub> , eV	Part, %	Bi 4f <sub>7/2</sub> , eV	Part, %	Pd:Bi
3:1	Pd <sup>0</sup> 334.5 Pd(II) <sub>ads</sub> 336.2	60.0 40.0	Bi <sup>0</sup> 156.5 Bi(III) 158.2	41.2 58.8	2.16
5:2	Pd <sup>0</sup> 334.5 Pd(II) <sub>ads</sub> 336.2	60.0 40.0	Bi <sup>0</sup> 156.6 Bi(III) 158.7	57.2 42.8	1.61
1:1	Pd <sup>0</sup> 334.4 Pd(II) <sub>ads</sub> 336.2	60.0 40.0	Bi <sup>0</sup> 157.1 Bi(III) <sub>ads</sub> 158.3	57.1 42.9	0.56
1:2	Pd <sup>0</sup> 334.4 Pd(II) <sub>ads</sub> 336.2	60.0 40.0	Bi(III) <sub>ads</sub> 157.6 Bi(III) 158.7	57.2 42.8	0.25

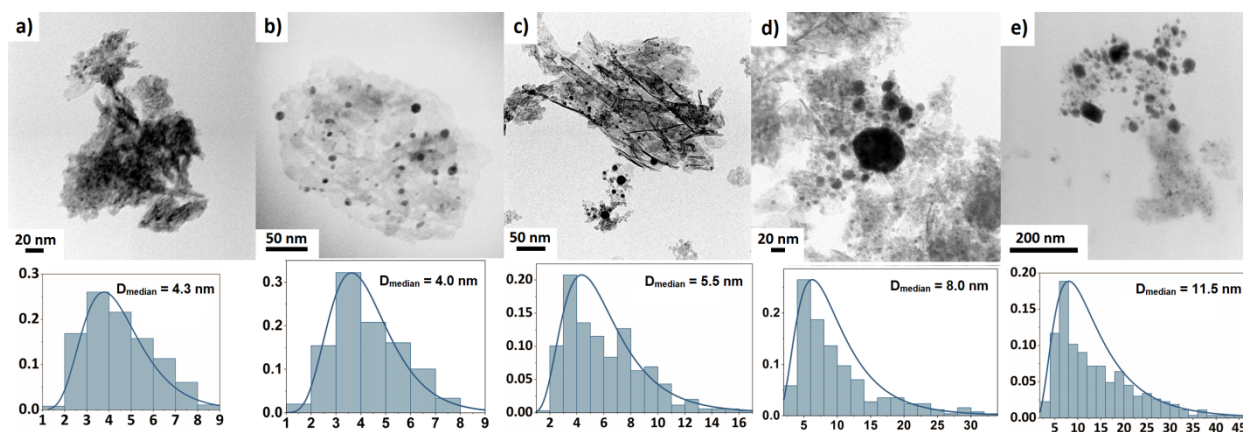


Fig. S1 – TEM images of Pd/Al<sub>2</sub>O<sub>3</sub> (a), Pd<sub>3</sub>:Bi<sub>1</sub>/Al<sub>2</sub>O<sub>3</sub> (b), Pd<sub>5</sub>:Bi<sub>2</sub>/Al<sub>2</sub>O<sub>3</sub> (c), Pd<sub>1</sub>:Bi<sub>1</sub>/Al<sub>2</sub>O<sub>3</sub> (d) and Pd<sub>5</sub>:Bi<sub>2</sub>/Al<sub>2</sub>O<sub>3</sub> samples (e)

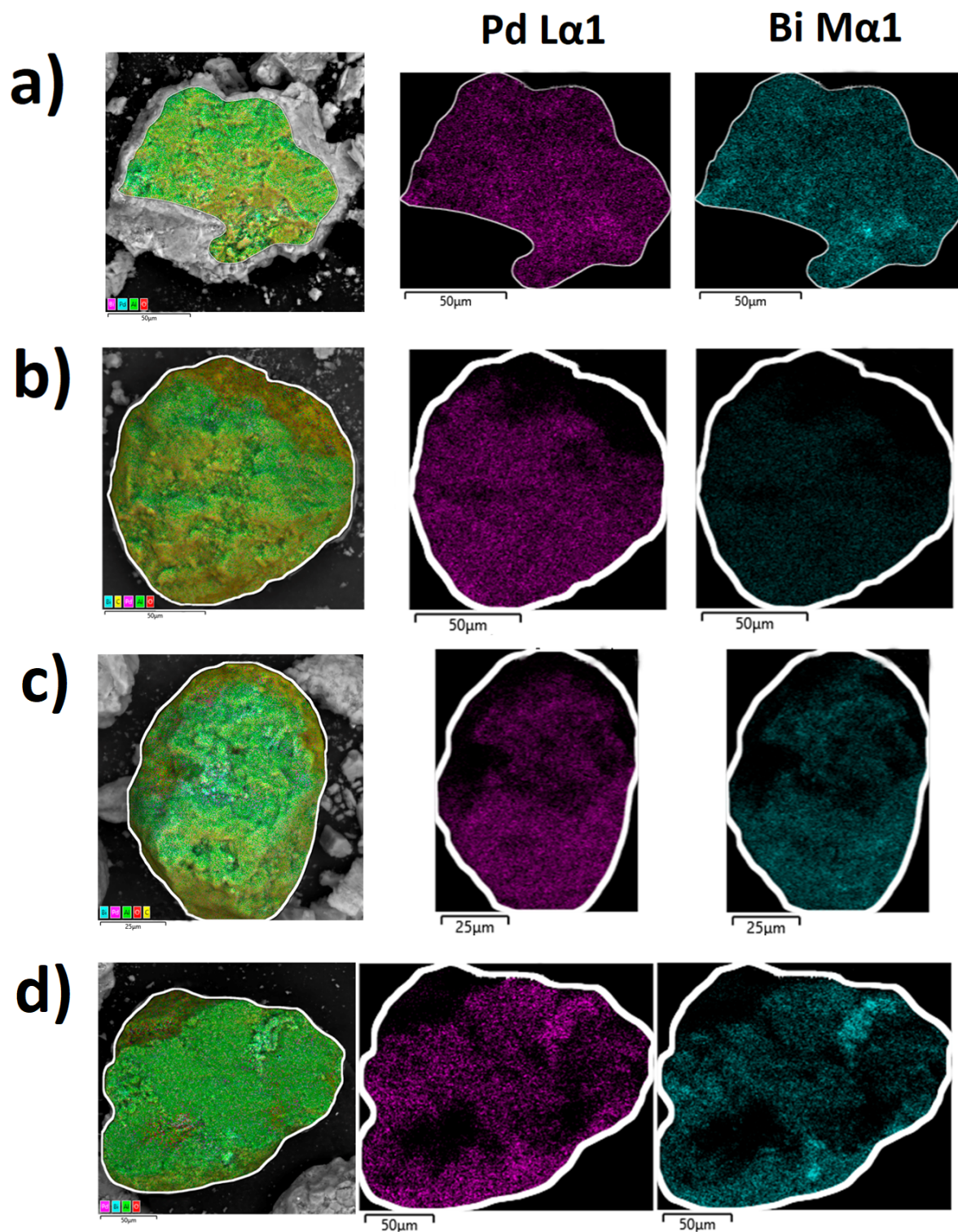


Fig. S2 – SEM-EDS images of Pd<sub>3</sub>:Bi<sub>1</sub>/Al<sub>2</sub>O<sub>3</sub> (a), Pd<sub>5</sub>:Bi<sub>2</sub>/Al<sub>2</sub>O<sub>3</sub> (b), Pd<sub>1</sub>:Bi<sub>1</sub>/Al<sub>2</sub>O<sub>3</sub> (c) and Pd<sub>5</sub>:Bi<sub>2</sub>/Al<sub>2</sub>O<sub>3</sub> samples (d)